PCCP

^{1}H–^{31}P CP/MAS NMR studies of mesostructured aluminophosphates†

Yaroslav Z. Khimyak and Jacek Klinowski

Department of Chemistry, University of Cambridge, Lensfield Road, Cambridge, UK CB2 1EW. E-mail: jk18@cam.ac.uk

Received 6th March 2001, Accepted 18th April 2001
First published as an Advance Article on the web 23rd May 2001

Mesostructured AlPO's with different structures synthesized *via* the cationic templating pathway have been characterized using ^{1}H–^{31}P cross-polarization/magic angle spinning (CP/MAS) NMR. Hexagonal (Hex) materials have much faster CP kinetics than lamellar (L) materials, which is reflected in shorter cross-polarization times (T_{PH}) and proton relaxation times in the rotating frame ($T_{1\rho H}$). T_{PH} increases with the increasing degree of condensation of the inorganic component, which is consistent with the increased ^{1}H–^{31}P distance. The CP dynamics of P sites connected to the surfactant head groups are affected by the fast motions of the protons in the $-N(CH_3)_3$ group. Measurements of $T_{1\rho H}$ indicate the microdomain structure of Hex-1, Hex-2 and L3, and two components with different proton relaxation rates have been identified. The fast relaxing component is attributed to protons within the inorganic network (mainly water molecules and OH groups coordinated to octahedral Al sites), while the component with the slower relaxation rate represents ^{1}H atoms at the inorganic/organic interface and from the organic component. The slower CP kinetics in mesolamellar AlPO's are caused by the particular structure of the inorganic network, consisting of tetrahedral Al with only a few protons located mainly at the inorganic/organic interface, that participates in the polarization transfer.

Introduction

^{1}H–^{31}P CP/MAS NMR has provided much new information on the microporous $AlPO_4$-*n* molecular sieves.[1–3] ^{1}H–^{31}P CP reveals the presence of water-rich and water-deficient domains in the gallophosphate molecular sieve cloverite, each contributing separately to the spectra.[4,5] ^{1}H–^{31}P CP NMR of human trabecular bone identifies three spectral components with intensities increasing at various rates.[6] ^{1}H–^{31}P CP/MAS can monitor the local environment of P atoms associated with different sources of protons (water molecules, organic molecules, surface P–OH and Al–OH groups *etc.*) and assign different lines in the spectra to the phosphate anions with various degrees of protonation.[7] Unfortunately, published ^{1}H–^{31}P CP/MAS spectra are often difficult to interpret. To reach reliable conclusions as to the origin of the changes in CP/MAS spectra in comparison with the single-pulse Bloch decay (BD) spectra, variable-contact-time (VCT) CP/MAS spectra must be measured.

CP is routinely used for the enhancement of the resolution and sensitivity of the spectra of nuclei with low natural abundance, by the polarization transfer from the abundant spins (typically ^{1}H) through the dipolar interaction.[8,9] The degree of signal enhancement depends on the distance between the protons and the target spins: the smaller the distance, the more efficient the cross-polarization. VCT experiments yield the characteristic time constant, T_{PH}, from which the relative internuclear distances can be estimated. The magnetization of ^{31}P depends on the contact time t_m according to[10,11]

$$M(t_m) = M_0(a_+ - a_-)^{-1}\left\{\exp\left(-\frac{a_- t_m}{T_{PH}}\right) - \exp\left(-\frac{a_+ t_m}{T_{PH}}\right)\right\} \quad (1a)$$

where

$$a_\pm = c(1 \pm \sqrt{1 - b/c^2}) \quad (1b)$$

$$b = (T_{PH}/T_{1\rho H})(1 + T_{PH}/T_{1\rho H}) + \varepsilon\alpha^2(T_{PH}/T_{1\rho P}) \quad (1c)$$

$$c = \tfrac{1}{2}(1 + \varepsilon\alpha^2 + T_{PH}/T_{1\rho H} + T_{PH}/T_{1\rho P}) \quad (1d)$$

and M_0 is the ^{31}P signal amplitude, T_{PH} is the cross-relaxation time between ^{31}P and ^{1}H, $T_{1\rho H}$ and $T_{1\rho P}$ are the ^{1}H and ^{31}P spin–lattice relaxation times in the rotating frame, $\varepsilon = N(^{31}P)/N(^{1}H)$ is the population ratio of the nuclei participating in the magnetization transfer, and $\alpha = \gamma_P B_{1P}/\gamma_H B_{1H}$ is the Hartmann–Hahn matching coefficient.

Direct comparison of published CP dynamics is often difficult, as different workers use different equations for data analysis. For example, a simplified form of eqn. (1) assuming $\varepsilon = 0$ and $T_{1\rho P} \gg T_{1\rho H}$ and $T_{1\rho H} \gg T_{PH}$ is often applied to obtain the CP dynamics parameters[6,12]

$$M(t_m) = M_0(1 - T_{PH}/T_{1\rho H})^{-1} \times [\exp(-t_m/T_{1\rho H}) - \exp(-t_m/T_{PH})] \quad (2)$$

For short contact times, t_m, magnetization increases with a time constant proportional to T_{PH}. At longer t_m, magne-

† Electronic Supplementary Information available. See http://www.rsc.org/suppdata/cp/b1/b102105m/

 DOI: 10.1039/b102105m

tization decreases with the time constant $T_{1\rho H}$, through ^1H relaxation in the rotating frame. The dipole–dipole constant, T_{PH}^{-1}, for the interaction between the ^1H and ^{31}P is proportional to r^{-6}, where r is the P–H distance.

Mesostructured AlPO's consist of the inorganic component arranged around the surfactant arrays with the structure resembling that of the surfactant mesophases. Mesolamellar AlPO's have been obtained using neutral,[13–15] anionic[16] or cationic[17–19] templating. We have described the synthesis of mesostructured AlPO's under ambient[20] and hydrothermal[21,22] conditions using cationic templating. The products are materials with lamellar or hexagonal mesostructures, and differ in the degree of ordering, extent of condensation of the inorganic arrays, relative content of the template and thermal stability. The differences in the structure of the inorganic component correspond to differences in organization of the surfactant arrays within the mesophases.[23] The diversity of mesostructured AlPO's offers a unique opportunity to compare products with the same or different mesostructure. Since the inorganic component of the mesostructured AlPO is known to be largely amorphous, XRD is of limited value for accurate structure determination. However, solid-state NMR is well suited for the study of such materials. ^1H–^{31}P CP/MAS NMR can justify the assignment of different lines to the specific structural units in mesostructured AlPO's, and provide important information on the structure of the inorganic/organic interface. Recently, mesolamellar AlPO obtained *via* anionic templating using dodecyl phosphate have been characterised by solid-state NMR techniques (^{31}P, ^1H and ^{27}Al MAS NMR and ^1H–^{31}P) 2D heteronuclear correlation spectroscopy (HETCOR) to differentiate between the phosphate group of the template and the inorganic framework.[24] In case of cationic templating, we have found that AlPO's with different mesostructures have significantly different ^1H–^{31}P CP kinetics. To the best of our knowledge no information on ^1H–^{31}P CP/MAS NMR of mesostructured AlPO's obtained *via* cationic templating is available in the literature.

Experimental

Samples were synthesized from an aqueous solution containing $Al(OC_3H_7^{iso})_3$, H_3PO_4 (85 wt.%), hexadecyl-trimethylammonium chloride (C_{16}TMACl) and tetramethylammonium hydroxide (TMAOH).[20–22] The composition of the synthesis mixtures and of the products is given in Table 1.

NMR spectra were recorded at 9.4 T using a Chemagnetics CMX-400 spectrometer. ^{31}P MAS spectra were measured at 161.89 MHz, $\pi/2$ (3.6 μs) pulses, 8 scans and 120 s recycle delays using zirconia rotors 4 mm in diameter spun in nitrogen at 8.0 kHz. ^{31}P chemical shifts are quoted with respect to an external 85% aqueous solution of H_3PO_4. ^{31}P CP/MAS NMR spectra were measured using zirconia rotors, 7.5 mm in diameter, spun in nitrogen at 5.5 kHz. VCT experiments were performed using ^1H $\pi/2$ pulse of 3.6 μs and 20 s repetition time, with contact time in the 0.01–24.0 ms range. Sixteen transients were accumulated. The Hartmann–Hahn condition was established using static $NH_4H_2PO_4$ and verified at the operating MAS rate.

$T_{1\rho H}$ and $T_{1\rho P}$ were determined in separate experiments. A modified CP pulse sequence, where a relaxation period, τ, is introduced between the beginning of the ^1H spin-lock condition and the beginning of the contact period (during which the Hartmann–Hahn condition is established) was used to determine $T_{1\rho H}$. Spin–lattice relaxation in the rotating frame of ^1H takes place during the period τ. The value of $T_{1\rho H}$ was determined from a plot of the intensity of the ^{31}P signal at the end of the contact period as a function of τ, using the equation of exponential decay. The $T_{1\rho P}$ for the target spin was determined as follows.[9,25] ^{31}P magnetization was first established by a CP procedure. Contact was then terminated by turning off the ^1H spin-lock. The ^{31}P magnetization, however, was held in the rotating frame for a variable time, τ, after which the remaining ^{31}P magnetization was sampled with dipolar decoupling of the ^1H spins. $T_{1\rho P}$ is the time constant of the decay of the ^{31}P magnetization in the rotating frame during τ. The ^1H–^{31}P polarization transfer used $t_m = 2.0$ ms. In the $T_{1\rho H}$ and $T_{1\rho P}$ experiments τ varied in the 0.05–20.0 ms range. The values of $T_{1\rho H}$ and $T_{1\rho P}$ were used for the determination of T_{PH} and ε from eqn. (1).

In view of the substantial peak overlap, the CP kinetics time constants were determined by analysing the peak intensities, without spectral deconvolution. This procedure has been adopted for numerous microporous AlPO molecular sieves, even when the spectra were much better resolved than ours.[3,5,26] Previous reports on CP dynamics in $AlPO_4$-*n* and related materials assumed that $T_{PH} \ll T_{1\rho H} \ll T_{1\rho P}$, and derived T_{PH} and $T_{1\rho H}$ directly from VCT experiments. However, mesostructured AlPO's show different trends. The values of $T_{1\rho H}$ measured in separate experiments[9,25] and those derived from VCT data using eqn. (2) are different. Thus, to obtain a full picture of the CP dynamics it is essential to perform VCT experiments to estimate T_{PH}, and to determine $T_{1\rho H}$ and $T_{1\rho P}$ using separate experiments. The data were analysed using eqn. (1) and (2). The parameters calculated from eqn. (2) are marked with asterisks (T_{PH}^*, $T_{1\rho H}^*$).

^{27}Al MAS NMR spectra were acquired at 104.20 MHz with pulses shorter than $\pi/10$ (0.3 μs pulse length). 1000 scans were acquired with a recycle time of 0.5 s. The position of the ^{27}Al resonances is quoted in ppm from external $Al(H_2O)_6^{3+}$.

Results

Mesostructured AlPO's

In the presence of tetraalkylammonium hydroxides, the supramolecular assembly in the AlPO–C_{16}TMACl system gives mesocomposites with different structures and properties. XRD identifies three hexagonal (Hex-1, Hex-2 and Hex-3) and three mesolamellar (L1, L2 and L3) products synthesized under different conditions (Table 2).[20–22] The inorganic component of different mesostructured AlPO's varies in the degree of condensation of the inorganic network, the P : Al ratio, and the population ratio of 6- and 4-coordinate Al sites (Table 2). In

Table 1 Chemical composition of the mesostructured products. Sample L2 was synthesised hydrothermally at 130 °C

	Synthesis mixture					Product			
Sample	Al_2O_3	P_2O_5	CTAC	TMAOH	H_2O	Al_2O_3	P_2O_5	$(CTA)_2O$	H_2O
Hex-1	1.00	2.02	0.83	4.40	320	1.00	1.21	0.666	5.75
Hex-2	1.00	2.02	0.50	5.02	320	1.00	1.15	0.816	6.52
L1a	1.00	3.05	0.50	8.11	350	1.00	1.62	1.15	3.62
L1b	1.00	3.03	0.83	7.28	340	1.00	1.60	0.994	5.77
L2	1.00	1.20	0.96	0.90	132.5	1.00	1.67	0.450	2.22
L3	1.00	2.02	0.50	6.20	330	1.00	1.28	1.26	7.24

Table 2 Properties of the inorganic component of the mesostructured products

Parameter	Mesolamellar AlPO	Hexagonal AlPO
Al(4) : Al(6)	L1, L2: Al(4) ≫ Al(6) L3: Al(6) > Al(4)	Al(6) > Al(4)
^{31}P MAS NMR chemical shift	L1, L2: from −17.0 to −31.0 ppm L3: from −1.0 to −19.0 ppm	from −1.0 to −19.0 ppm
Degree of condensation	L2 > L1 > L3	Hex-1 > Hex-2 > Hex-3
P : Al ratio	L1, L2: P : Al > 1.50 L3: P : Al ≈ 1.30	P : Al = 0.70–1.30
Content of organic component	L2 < L1 < L3	Hex-1 < Hex-2 < Hex-3
Thermal stability	L2 > L1 > L3	Hex-1 > Hex-2 > Hex-3

mesolamellar L2 the inorganic component is the most condensed, and in L1 and L2 aluminium is predominantly 4-coordinate. By contrast, in L3 aluminium is mostly 6-coordinate.

The content of $C_{16}TMA^+$ cations, the only organic species in the products, is governed by: (1) the P_2O_5 : Al_2O_3 ratio in the synthesis mixture (henceforth abbreviated as P/A); (2) the surfactant content; (3) the P : Al ratio in the mesocomposites; and (4) the pH.[23] Thus, increasing the P/A during the synthesis of Hex increases both the P : Al ratio in the products and the surfactant content. The latter also increases with increased pH. The differences between the mesocomposites are also reflected in the specific organization of the surfactant arrays. Thus, at ambient temperatures Hex-1, Hex-2 and L2 show predominant *gauche* disordered conformation of the aliphatic chains, while in L1 and L3 they are in the all-*trans* conformation.

^{31}P MAS NMR

^{31}P MAS NMR spectra of mesostructured AlPO's synthesised under ambient conditions contain several resonances in the range from −0.1 to −21.0 ppm, indicating the presence of 4-coordinate P surrounded by the surfactant cations, interlayer water and Al(4) and Al(6) atoms.[20] The sharp peak at −0.8 ppm in the spectrum of Hex-1 (Fig. 1) comes from the interfacial P atoms attached to the surfactant, and the broad resonance with a maximum between 8.0 and −12.0 ppm represents several sites with different degrees of condensation. Hex-1 can be considered to be made of the $P(OAl(4))_x(OAl(6))_y(OH)_{[4-(x+y)]}$ units. Substitution of OH groups by Al(6) units and an increased population of the Al(4) units in the first coordination sphere of P result in the upfield shift of the ^{31}P peaks. Sites in which P is connected to four Al(4) tetrahedra are absent from Hex-1. The relative intensity of the peak at −0.8 ppm increases with the increased surfactant content and increased P/A. With increased pH the maximum of the broad resonance shifts from −13.0 to −8.0 ppm.

^{31}P NMR spectra of Hex-2 show an increased contribution of the peaks at low field, indicating more sites where P is attached to the surfactant cations, consistent with higher template content in the mesocomposite. A shoulder at −3.5 ppm is present, in addition to the peak at *ca.* −1.0 ppm, and higher field resonances at −7.5, −11.0, −15.0 and −19.0 ppm. The deconvoluted spectra are given as Electronic Information.† Generally, the different sites become more distinct with increased water content and P/A. Thus, Hex-2 obtained at low water content and P/A < 2.00 still has a high proportion of P sites between −7.0 and −18.0 ppm. A higher water content and P/A increase the contribution of sites at > −3.7 ppm.

L1 give ^{31}P MAS NMR spectra with well-resolved peaks between −17.8 and −21.5 ppm (Fig. 2). The differences between L1a and L1b are related to the different coordination of P to water.[21,22] After dehydration at 110 °C the spectra of L1a and L1b are identical and consist of a single resonance at −19.0 ppm. The ^{31}P MAS NMR spectra of L1 are consistent with the presence of $P(OAl)_3OR$, R = H or $C_{16}TMA^+$ units.

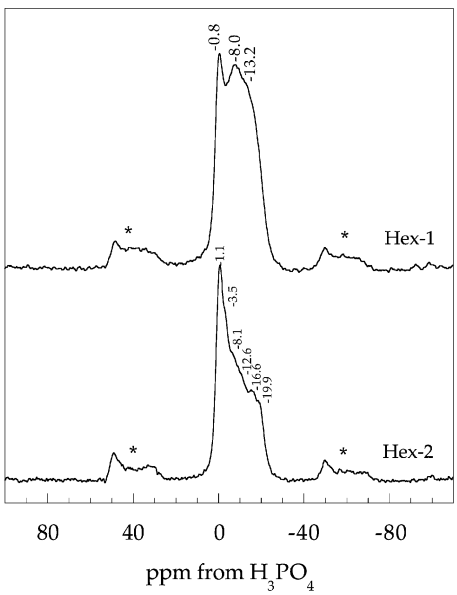

Fig. 1 ^{31}P MAS NMR spectra of Hex-1 and Hex-2 AlPO's.

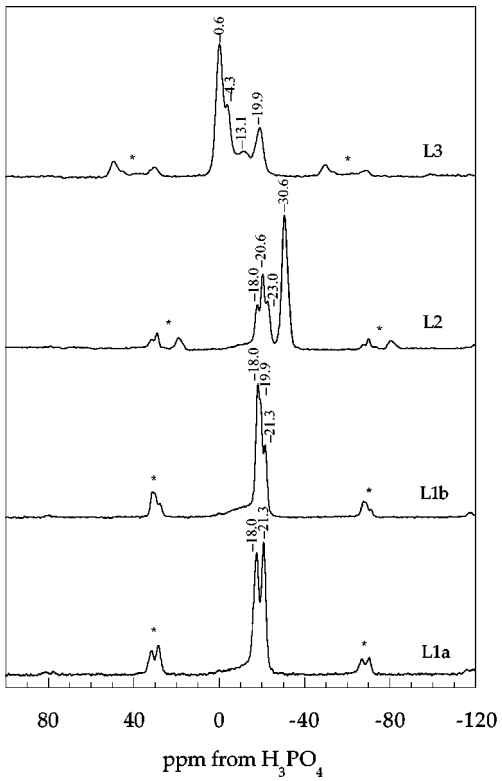

Fig. 2 ^{31}P MAS NMR spectra of mesolamellar AlPO's.

Phosphate tetrahedra are dominant at the inorganic/organic interface and bond electrostatically to the surfactant cations.

L3 has an increased contribution of low-field ^{31}P resonances which resembles that of Hex-3, indicating a similar structure of the surfactant/inorganic interface. We note that XRD indicates that the material contains some L1. The contribution of the sites with chemical shifts below −19.0 ppm is greater than for Hex-3, and the spectrum is different from those of L1a and L1b. The only similarity is the peak at −19.0 ppm, which can be partly attributed to the L1 impurity. In the spectra of L1a and L1b there are 2–3 distinct resonances at *ca.* −19 ppm. L3 gives only a broad resonance, indicating that L1 co-precipitating with L3 is less ordered than pure L1.

The main feature of the ^{31}P spectrum of L2 is the peak at −30.7 ppm assigned to P coordinated to four AlO_4 tetrahedra. Several overlapping peaks are found at −18.0, −20.5 and −22.8 ppm, all from 4-coordinate P, most probably to three Al atoms. The fourth oxygen may be bonded to hydrogen, water or the surfactant. The broad low intensity peak at −13.8 ppm comes from amorphous impurities.[21,22]

The inorganic component of Hex is much less condensed and less well ordered, as evidenced by the predominantly octahedral coordination of Al and broad low-field ^{31}P peaks. Hexagonal AlPO's are progressively less well condensed as the pH of the synthesis mixtures increases, in the sequence Hex-1 > Hex-2 > Hex-3. While L1 and L2 can be considered as semi-crystalline with fairly well organised inorganic networks,[21,22] the inorganic component in Hex is largely amorphous.

^{1}H–^{31}P CP/MAS

Hexagonal aluminophosphates. VCT CP/MAS spectra (Fig. 3) reveal different CP kinetic behaviours for P sites with different degrees of condensation (Table 3). For both Hex-1 and Hex-2, the values of $T^{*}_{1\rho H}$ and $T_{1\rho H}$ are clearly different, suggesting that the assumptions inherent in eqn. (2) cannot be applied. Nevertheless, results of Fit I will also be discussed, since a number of reports on ^{1}H–^{31}P CP dynamics in related systems are based on eqn. (2).[6,12]

For Hex-1 the broad line at *ca.* −8 ppm has faster CP kinetics than the narrow peak at −0.89 ppm. As a result, in the CP/MAS spectra registered with short contact times (t_m < 1.0 ms), the line at −0.89 ppm is less intense than in the BD spectra. The CP kinetics of Hex-2 is similar to that of Hex-1 (Fig. 4). The resonance corresponding to the P site with the lowest degree of condensation has slower CP kinetics than the lines at higher field. For Hex-1 and Hex-2, the $T_{1\rho H}$ measurements reveal a structural inhomogeneity, as the I–τ dependence is biexponential (Fig. 4). Two microdomains are present with different ^{1}H relaxation times (Table 3).

The degree of condensation of P sites has a significant influence on ^{31}P relaxation in the rotating frame. Hex-1 sites resonating above −13.5 ppm have $T_{1\rho P}$ < 31.4 ms with the longest $T_{1\rho P}$ corresponding to the site at −0.89 ppm. For the

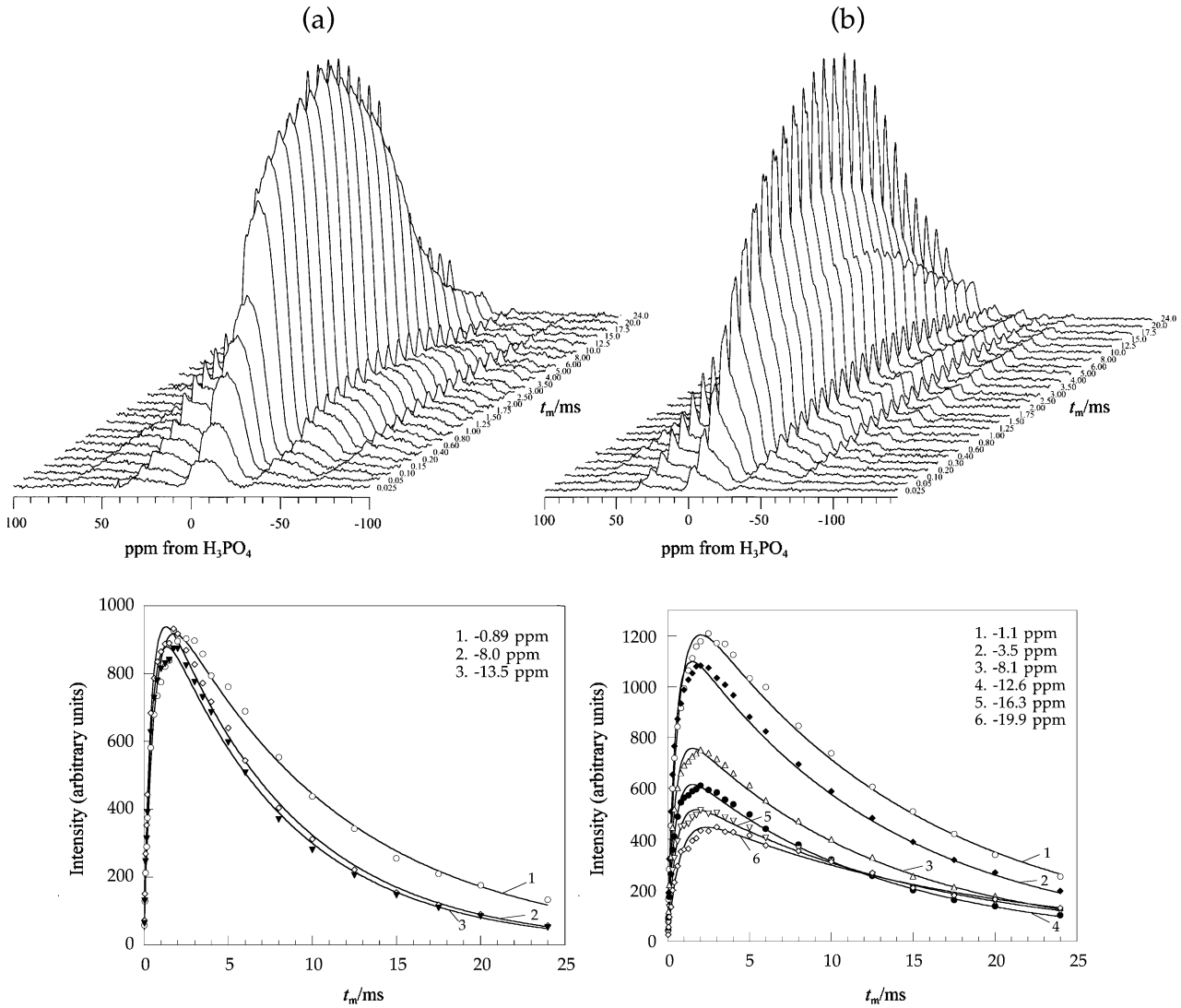

Fig. 3 VCT ^{1}H–^{31}P CP/MAS spectra of Hex-1 (a) and Hex-2 (b) and the dependence of the intensity of different peaks on the contact time.

Table 3 (a) $T_{1\rho H}$ and $T_{1\rho P}$ relaxation times of hexagonal AlPO's

		$T_{1\rho H}$/ms						
Sample	$-\delta$/ppm	Average	R^2	Fast component	Slow component	R^2	$T_{1\rho P}$/ms	R^2
Hex-1	0.89	4.66 ± 0.27	0.983	1.29 ± 0.27	6.49 ± 0.71	0.995	31.4 ± 1.4	0.977
	8.0	3.94 ± 0.17	0.991	1.25 ± 0.15	5.40 ± 0.42	0.999	26.5 ± 0.8	0.991
	13.5	3.97 ± 0.15	0.993	1.40 ± 0.14	5.42 ± 0.30	0.999	30.2 ± 0.6	0.996
Hex-2	1.1	5.60 ± 0.27	0.987	1.25 ± 0.12	7.58 ± 0.37	0.999	37.8 ± 1.5	0.984
	3.5	5.39 ± 0.29	0.984	1.12 ± 0.08	7.47 ± 0.34	0.999	32.7 ± 1.0	0.984
	8.1	5.07 ± 0.28	0.984	1.18 ± 0.07	7.32 ± 0.32	0.999	33.4 ± 1.1	0.989
	12.6	4.95 ± 0.29	0.983	1.03 ± 0.10	6.91 ± 0.31	0.998	33.8 ± 1.4	0.982
	16.3	5.29 ± 0.31	0.982	1.14 ± 0.15	7.35 ± 0.35	0.998	44.4 ± 2.3	0.971
	19.9	5.84 ± 0.32	0.983	1.20 ± 0.18	7.83 ± 0.35	0.998	62.5 ± 5.7	0.909

(b) CP kinetics parameters of hexagonal AlPO's

		Fit I[a]			Fit II[b,c]		
Sample	$-\delta$/ppm	T^*_{PH}/ms	$T^*_{1\rho H}$/ms	R^2	T_{PH}/ms	ε	R^2
Hex-1	0.89	0.596 ± 0.031	10.49 ± 0.46	0.985	1.80 ± 0.13	1.85 ± 0.24	0.985
	8.0	0.428 ± 0.017	7.66 ± 0.18	0.993	1.03 ± 0.05	1.31 ± 0.12	0.994
	13.5	0.456 ± 0.017	7.59 ± 0.22	0.994	1.03 ± 0.05	1.12 ± 0.10	0.994
Hex-2	1.1	0.623 ± 0.030	14.04 ± 0.41	0.985	2.27 ± 0.16	2.47 ± 0.29	0.986
	3.5	0.431 ± 0.020	12.53 ± 0.34	0.988	1.48 ± 0.10	2.38 ± 0.24	0.989
	8.1	0.440 ± 0.017	12.24 ± 0.29	0.991	1.52 ± 0.08	2.36 ± 0.20	0.992
	12.6	0.450 ± 0.017	11.86 ± 0.26	0.992	1.50 ± 0.08	2.22 ± 0.18	0.993
	16.3	0.508 ± 0.021	14.49 ± 0.38	0.989	1.94 ± 0.11	2.70 ± 0.24	0.990
	19.9	0.726 ± 0.036	16.50 ± 0.56	0.983	2.72 ± 0.19	2.63 ± 0.30	0.984

[a] Fit I corresponds to eqn. (2). [b] Fit II corresponds to eqn. (1). [c] $T_{1\rho H}$ and $T_{1\rho P}$ in (a) were used to determine the T_{PH} and ε in the fitting.

same range of chemical shifts, the $T_{1\rho P}$ in Hex-2 is longer (32.7–37.8 ms). Hex-2 sites resonating at higher field have longer $T_{1\rho P}$. Slower relaxation explains the increased contribution of the P sites below −13.5 ppm in the CP/MAS NMR spectra with long t_m.

For Hex, the scaling factor ε, determined from eqn. (1), is larger than 1.0, indicating that polarization is transferred from one proton to more than one ^{31}P. It is clear that only a limited number of protons from those present participate in CP. For the sites at the lowest field in Hex-1 (at −0.89 ppm) and Hex-2 (−1.1 and −3.5 ppm), ε is larger than for the sites with a slightly higher degree of condensation.

The use of eqn. (2) leads to different CP time constants. To assess the validity of the values from Fit II *vis-à-vis* those from Fit I, it is necessary to compare T^*_{PH} and $T^*_{1\rho H}$ with T_{PH}/a_- and T_{PH}/a_+.[1] For Hex, the comparison shows the difference to be within 5.0–7.0% for all P sites. Even though the T^*_{PH} obtained from eqn. (2) are much lower than the T_{PH} determined using the more elaborate equation, the changes in the CP time constants follow the same trend.

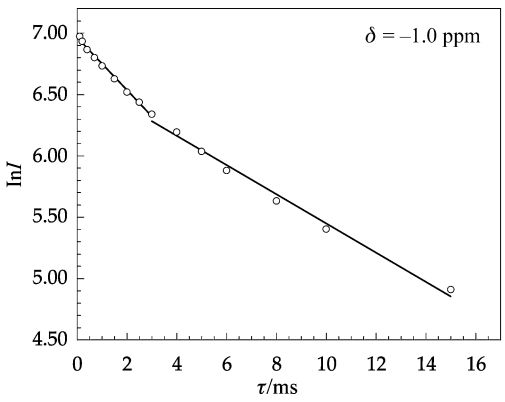

Fig. 4 Semilogarithmic dependence of the intensity of the peak at −1.0 ppm for Hex-2 on the holding time in the $T_{1\rho H}$ experiment.

Mesolamellar AlPO's. The CP kinetics in L are much slower than in Hex (Table 4). While the maximum of the CP signal corresponds to t_m = 1–2 ms for Hex-1 and Hex-2, in L it is found at t_m = 4–5 ms. In contrast to Hex, the CP dynamics of L are difficult to fit using either eqn. (1) or (2), probably due to slow CP kinetics with a relatively small decay in the intensity of the peaks, even at the longest contact times.

For L1a, the two main resonances at −18.0 and −21.2 ppm both have T^*_{PH} = 1.32 ms. Fit II gives much larger values of the time constants, with $T_{PH} \geqslant 6.91$ ms and $\varepsilon > 4.5$. L1b shows even slower CP dynamics. T_{PH} is comparable to that for L1a (ε = 4.0 was used in the fittings). A broad peak at −13.0 ppm in both L1a and L1b appears at short contact times, and has much faster CP kinetics, proving that it corresponds to the amorphous impurities.

For L2 (Fig. 5(a)), with the most condensed inorganic component, T^*_{PH}, increases from 1.03 to 1.74 ms, while the chemical shift changes from −18.0 to −31.0 ppm. The trend of change of T_{PH} obtained using eqn. (1) is similar to that for T^*_{PH}. However, the absolute values of T_{PH} are much longer, and the scaling factor ε = 3.41–4.46 is much larger than for Hex.

For L3 (Fig. 5(b)), the P sites at low field (−0.58 and −4.3 ppm) have CP dynamics resembling those in Hex-2. Thus, the sites with the lowest degree of condensation have slower CP kinetics than the nearest upfield site. ^{31}P sites at high field have substantially longer T_{PH} (4.62 ms for the line at −13.0 ppm and T_{PH} = 8.57 ms for the line at −19.4 ppm).

The $T_{1\rho H}$ in L is larger than in Hex. For the different sites in L1a and L1b there is practically no variation in $T_{1\rho H}$. L2 has faster $T_{1\rho H}$ relaxation (6.80–9.08 ms). In L3, the P sites at −0.58 and −4.3 ppm have a biexponential I–τ_d dependence, and two microdomains with different rates of ^{1}H relaxation are detected (Table 4(a)).

Analysis of $T_{1\rho P}$ for L is less straightforward. For L1a, L1b and L3, the $T_{1\rho P}$ is longer than those for Hex. In L1a and L1b, $T_{1\rho P} \approx 50.0$ ms, and for L1b relaxation is even slower. For L3, $T_{1\rho P}$ is very long for sites resonating at −0.58, −13.5 and −19.0 ppm. The site at −4.3 ppm appears to be more mobile

Table 4 (a) $T_{1\rho H}$ and $T_{1\rho P}$ relaxation times for mesolamellar AlPO's

		$T_{1\rho H}$/ms						
Sample	$-\delta$/ppm	Average	R^2	Fast component	Slow component	R^2	$T_{1\rho P}$/ms	R^2
L1a	18.0	14.14 ± 0.42	0.983	—	—	—	53.2 ± 3.1	0.962
	21.3	14.14 ± 0.49	0.993	—	—	—	49.3 ± 2.5	0.972
L1b	18.5	17.57 ± 0.52	0.991	—	—	—	63.0 ± 2.5	0.982
	19.9	17.33 ± 0.66	0.986	—	—	—	39.8 ± 1.4	0.986
	22.3	17.64 ± 0.88	0.975	—	—	—	74.5 ± 6.2	0.922
L2	18.3	9.08 ± 0.58	0.979	—	—	—	27.1 ± 1.3	0.982
	21.3	7.10 ± 0.31	0.991	—	—	—	36.3 ± 0.9	0.971
	23.3	7.01 ± 0.31	0.991	—	—	—	53.5 ± 1.5	0.909
	31.4	6.70 ± 0.30	0.981	—	—		47.5 ± 1.9	0.965
L3	0.58	12.76 ± 0.59	0.982	1.60 ± 0.36	15.42 ± 0.65	0.997	77.4 ± 4.9	0.954
	4.3	12.87 ± 0.69	0.976	1.37 ± 0.19	16.17 ± 0.59	0.998	31.4 ± 1.3	0.981
	13.1	13.92 ± 0.54	0.987	—	—		76.7 ± 10.3	0.824
	19.4	17.52 ± 0.89	0.976	—	—		262.5 ± 61.6	0.589

(b) ^{1}H–^{31}P CP kinetics parameters for mesolamellar AlPO's

		Fit I[a]			Fit II[b,c]		
Sample	$-\delta$/ppm	T^*_{PH}/ms	$T^*_{1\rho H}$/ms	R^2	T_{PH}/ms	ε	R^2
L1a	18.0	1.32 ± 0.07	28.7 ± 1.3	0.981	6.91 ± 1.89	4.52 ± 1.73	0.984
	21.3	1.32 ± 0.06	28.0 ± 1.2	0.982	7.22 ± 2.13	4.73 ± 1.92	0.984
L1b	18.5	1.07 ± 0.11	63.7 ± 7.4	0.934	7.08 ± 0.88	4.0	0.910
	19.9	0.853 ± 0.071	71.4 ± 10.5	0.956	6.89 ± 0.89	4.0	0.903
	22.3	1.32 ± 0.13	60.6 ± 14.1	0.937	8.12 ± 0.94	4.0	0.923
L2	18.3	1.03 ± 0.06	20.8 ± 0.8	0.977	5.50 ± 0.36	3.85 ± 0.37	0.972
	21.3	1.49 ± 0.06	17.9 ± 0.5	0.988	7.20 ± 0.72	3.41 ± 0.58	0.989
	23.3	1.64 ± 0.06	21.4 ± 0.5	0.990	8.70 ± 0.72	3.76 ± 0.55	0.991
	31.4	1.74 ± 0.08	25.8 ± 0.9	0.983	11.97 ± 0.68	4.46 ± 0.33	0.982
L3	0.58	0.887 ± 0.047	24.1 ± 1.0	0.981	2.35 ± 0.23	1.77 ± 0.33	0.983
	4.3	0.404 ± 0.025	20.0 ± 0.8	0.980	1.23 ± 0.22	2.11 ± 0.60	0.981
	13.1	0.929 ± 0.075	29.1 ± 1.2	0.958	4.62 ± 1.37	4.98 ± 2.02	0.968
	19.4	1.58 ± 0.11	48.1 ± 4.7	0.967	8.57 ± 3.36	5.21 ± 2.83	0.969

[a] Fit I corresponds to eqn. (2). [b] Fit II corresponds to eqn. (1). [c] $T_{1\rho H}$ and $T_{1\rho P}$ in (a) were used to determine the T_{PH} and ε in the fitting.

($T_{1\rho P}$ = 31.4 ms, comparable to Hex). The sites with a low degree of condensation in L2 have fairly short $T_{1\rho P}$. For the sites at −23.3 and −31.4 ppm, $T_{1\rho P}$ is much longer (54.4 and 48.5 ms, respectively).

Discussion

^{1}H–^{31}P CP/MAS NMR shows substantial differences in the build-up of ^{31}P magnetization in different aluminophosphates upon the transfer of polarization from different proton sources. It has been suggested that protons from the extra-framework water occluded in the channels of $AlPO_4$-*n* are too mobile at room temperature to transfer polarization efficiently to ^{31}P nuclei.[1] This leaves protons in the organic template, coordinated water molecules and hydroxy groups connected either to P or Al to act as the CP sources. In VPI-5, CP proceeds mainly from the protons of the less mobile water, coordinated to the Al atoms.[1–3] In cloverite, CP takes place within the P–OH groups and T_{PH} is very short.[4,5] In $AlPO_4$-41 the CP is governed by two processes with different time constants. For this material CP dynamics singles out the interactions between the template molecules and the framework nuclei,[26] while Hartmann *et al.* described differences in CP dynamics of the various P sites in terms of different degrees of protonation of the phosphate anions.[12]

In Hex the T_{PH} is quite short (0.90–2.72 ms), indicating that the P atoms are close to the protons. Polarization transfer may thus be thought of as occurring within the P–OH bonds. This is justified by the substantial contribution of P sites with a low degree of condensation. The influence of water molecules coordinated to Al must also be taken into account, as the inorganic network consists predominantly of highly hydrated Al(6) sites. An increase in T_{PH} for sites resonating at higher field is clearly related to the increased distance between the P atoms and the source of protons, an effect observed for VPI-5[1,3] and MCM-41.[27] In MCM-41, the T_{SiH} increases from 1.3 to 2.1 ms with the increased condensation of the inorganic network, composed mainly of Q^3 and Q^4 silicate units.[27] This also indicates the absence of sources of protons in the bulk of the inorganic component which may be attributed to the increased content of Al(4) units away from the organic-inorganic interface. However, the T_{PH} for sites with the largest chemical shift in Hex (−0.89 ppm for Hex-1 and −1.1 ppm for Hex-2) are longer than those for sites with a higher degree of condensation. This confirms the assignment of the former units to the P atoms connected to the surfactant headgroups. The slower CP kinetics results from the fact that, in addition to the protons from the hydroxy groups or water molecules coordinated to Al atoms (these are already further from P atoms than the protons of P–OH groups), CP may proceed from fairly mobile protons of the surfactant headgroups.[23] The changed mobility of the ^{1}H source for the downfield P sites in Hex-1 and Hex-2 is also illustrated by a change in $T_{1\rho H}$, which is longer than for the sites with a higher degree of condensation.

L1 and L2 have substantially longer T_{PH}. For L3, the T_{PH} for the sites with a low degree of condensation is comparable to those for Hex, while the T_{PH} for the P sites resonating at a higher field is similar to those for L1 and L2. It is clear that the proton source in L1 and L2 is much further from the P atoms than in Hex. This is consistent with a higher degree of condensation of the inorganic network in L, and hence a lower content of P–OH groups. The environment of Al in L is also different, as Al(4) is dominant and practically no coordinated water is present in the framework. As a result, CP pro-

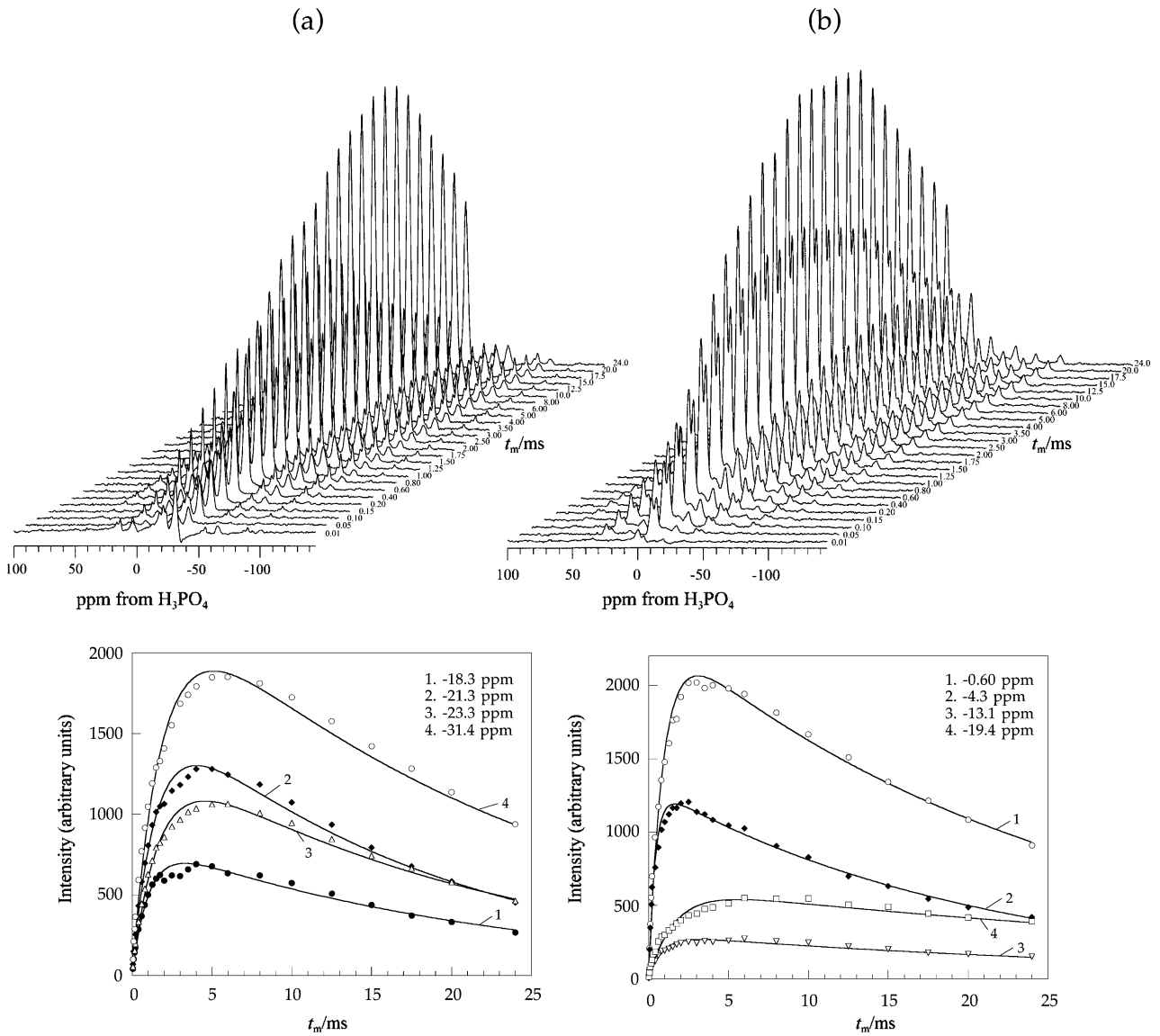

Fig. 5 VCT ^1H–^{31}P CP/MAS spectra of L2 (a) and L3 (b) and the dependence of the intensity of different peaks on the contact time.

ceeds mainly from surfactant species and remote water molecules. As in Hex, T_{PH} increases with the increasing degree of condensation of the inorganic framework. The difference in CP dynamics of the inequivalent sites in L1a and L1b is small, confirming the similarity of the two structures. By contrast, the substantial increase in the degree of condensation of the P sites in L2 is accompanied by a significant increase in T_{PH}. The resonance at −31.0 ppm is assigned to $P(OAl)_4$, and therefore P does not have nearby protons which would enable efficient polarization transfer. In fact, ^1H–^{31}P CP/MAS lines are observed even at the shortest t_m. This is due to ^{31}P spin diffusion from the adjacent $P(OAl)_3OR$ (R = H or $N(CH_3)_3C_{16}H_{33}$) sites. A similar phenomenon was observed for the $P(OGa)_4$ units in the ^1H–^{31}P CP/MAS spectrum of cloverite.

The $T_{1\rho H}$ in mesostructured AlPO's varies in the 3.4–17.8 ms range. The $T_{1\rho H}$ relaxation depends on fluctuations in the magnetic field of the protons caused by their motion. $T_{1\rho H}$ is known to be a volume property and is averaged over a distance of *ca.* 2 nm by spin diffusion.[9,28] This is confirmed for mesostructured AlPO's, for which small differences are found in $T_{1\rho H}$ for different P sites in the same structure. The relationship between the $T_{1\rho H}$ and the mobility of the protons responsible for the CP is not straightforward, mainly because of the very efficient ^1H spin diffusion averaging the differences between the protons. All the same, $T_{1\rho H}$ remains an important structural parameter, and differs greatly for different mesostructured AlPO's. It is clear that in Hex the proton reservoir is much more mobile than in L, since the $T_{1\rho H}$ is much smaller. This is also consistent with the trends of the mobility of the incorporated template.[23] In Hex-1 $T_{1\rho H}$ is shorter than in Hex-2, which can, in part, be explained by the larger content of the template in Hex-2, and a less condensed inorganic network with much higher contribution of the P sites connected to the surfactant headgroups. The measurements of $T_{1\rho H}$ reveal the structural heterogeneity of Hex and L3, as domains with slightly different rates of proton relaxation are detected. This effect is observed for the mesocomposites with predominantly octahedral coordination of Al. It seems that the protons in the inorganic component contribute differently to the CP dynamics than those located at the inorganic/organic interface or within the organic component. The former are responsible for the fast-relaxing $T_{1\rho H}$ component, while the latter constitute the slow-relaxing component.

In L, $T_{1\rho H}$ is longer than 14.0 ms for L1a, L1b and L3, and in the 6.70–9.08 ms range for L2. The main source of the CP in L is different from that in Hex. However, the significant difference between $T_{1\rho H}$ in L1a,b and L2 suggests that, besides differences in the structure of the inorganic component, the inorganic/organic interface is also different, for example with

respect to the mobility of the surfactant headgroups connected to the P atoms. This effect has also been observed in the ^{1}H–^{13}C CP/MAS dynamics.[23] The values of $T_{1\rho H}$ suggest that the source protons in L2 are much more mobile than in L1a,b and L3. As in Hex, the relaxation of protons cross-polarizing with low-field ^{31}P sites in L3 is inhomogeneous.

The scaling factor ε is larger than 1.0, and is larger for L (>3.5) than for Hex (1.1–2.7). The larger scaling factor indicates an increased number of P atoms receiving polarization from a single proton for L compared to Hex, which proves participation of the ^{1}H atoms from within the inorganic component in the polarization transfer in the latter. Unfortunately, there are few published results on the T_{CP} and ε in porous AlPO's. Blasco *et al.* found $\varepsilon \approx 2$ in microporous VPI-5.[1] Caldarelli *et al.* used eqn. (1) for the analysis of ^{1}H–^{31}P CP dynamics of $AlPO_4$-41 assuming $\varepsilon = 1$.[26] Our results suggest that only a small number of protons transfer polarization to ^{31}P. A comparison of the ^{1}H–^{31}P CP/MAS dynamics in mesostructured AlPO's with published results on ^{1}H–^{29}Si CP/MAS dynamics in mesostructured silicates obtained *via* the cationic templating pathway,[27] shows much more significant differences between AlPO's than between the silicates with different mesostructures. Thus, the T_{SiH} for the Q^3 sites is similar for the lamellar, cubic and hexagonal silicates, and is in the 1.0–1.5 ms range. The same applies to the Q^4 sites with $T_{SiH} = 2.0$–2.1 ms. Different $T_{1\rho H}$ were found only for cubic silicates (5 ms), and for hexagonal and lamellar materials (9 ms). This is not surprising, since the different structure of the inorganic component in materials with different symmetry is reflected in the variation of the Q^3/Q^4 ratio only within the 0.59–0.96 range. In the AlPO's, the mesostructure change from Hex to L is accompanied by a much more significant change in the degree of condensation and coordination of P and Al, leading to a large variation in T_{PH}, $T_{1\rho H}$ and $T_{1\rho P}$, even within the same mesostructure. It appears that the CP time constants in the Hex are comparable to those for mesostructured silicates, while L1 and L2 have much longer T_{PH} and $T_{1\rho H}$, with the former similar to that in VPI-5 and $AlPO_4$-41.

Conclusions

Mesostructured AlPO's synthesized *via* the cationic templating pathway have been characterized using ^{1}H–^{31}P CP/MAS NMR. Materials with different mesostructures have significantly different CP dynamics, which originate from the differences in the structure of the inorganic component, proton reservoir and inorganic/organic interface, and in the mobility of the organic component.

Hexagonal materials have much faster CP kinetics than lamellar products. The distance between ^{31}P and ^{1}H in Hex-1 and Hex-2 is smaller than in L. T_{PH} cross-polarization time increases with increasing degree of condensation of the inorganic component, which is consistent with the increasing ^{1}H–^{31}P distance. This is the case for all P atoms in Hex-1 and Hex-2, except those with the lowest degree of condensation. These atoms are connected to the surfactant head groups, and the CP dynamics are affected by the fast motions of the protons in the $-N(CH_3)_3$ group. Measurements of $T_{1\rho H}$ show that the proton reservoir in Hex-1, Hex-2 and L3 consists of two microdomains contributing differently to CP kinetics. The fast relaxing component is attributed to protons within the inorganic network (mainly water molecules and OH groups coordinated to octahedral Al sites).

The slower CP kinetics in mesolamellar AlPO's are caused by the differences in the inorganic network. This consists of tetrahedral Al with only a few protons, located mainly at the inorganic/organic interface, to participate in the polarization transfer.

Acknowledgements

We are grateful to the Cambridge Oppenheimer Fund for the Research Fellowship for Y.K.

References

1 T. Blasco, J. Perez-Pariente and W. Kolodziejski, *Solid State NMR*, 1997, **8**, 185.
2 H. Y. He, W. Kolodziejski and J. Klinowski, *Chem. Phys. Lett.*, 1992, **200**, 83.
3 W. Kolodziejski, H. Y. He and J. Klinowski, *Chem. Phys. Lett.*, 1992, **191**, 117.
4 W. Kolodziejski and J. Klinowski, *Chem. Phys. Lett.*, 1997, **266**, 597.
5 W. Kolodziejski and J. Klinowski, *J. Phys. Chem. B*, 1997, **101**, 3937.
6 A. Kaflak, D. Chmielewski, A. Górecki and W. Kolodziejski, *Solid State NMR*, 1998, **10**, 191.
7 H. Nakayama, T. Eguchi, N. Nakamura, S. Yamaguchi, M. Danjyo and M. Tsuhako, *J. Mater. Chem.*, 1997, **7**, 1063.
8 D. Michel and F. Engelke, in *Solid-State NMR III, NMR Basic Principles and Progress*, ed. P. Diehl, Springer-Verlag, Berlin, 1994, vol. 32, p. 69.
9 R. Voelkel, *Angew. Chem., Int. Ed. Engl.*, 1988, **27**, 1468.
10 M. Mehring, *Principles of High-Resolution NMR in Solids*, Springer-Verlag, Berlin, 1983.
11 T. H. Walter, G. L. Turner and E. Oldfield, *J. Magn. Reson.*, 1988, **76**, 106.
12 M. Hartmann, A. M. Prakash and L. Kevan, *J. Chem. Soc., Faraday Trans.*, 1998, **94**, 723.
13 S. Oliver, A. Kuperman, N. Coombs, A. Lough and G. A. Ozin, *Nature*, 1995, **378**, 47.
14 A. Sayari, I. Moudrakovski, J. S. Reddy, C. I. Ratcliffe, J. A. Ripmeester and K. F. Preston, *Chem. Mater.*, 1996, **8**, 2080.
15 Q. M. Gao, J. S. Chen, R. R. Xu and Y. Yue, *Chem. Mater.*, 1997, **9**, 457.
16 M. Froba and M. Tiemann, *Chem. Mater.*, 1998, **10**, 3475.
17 T. Kimura, Y. Sugahara and K. Kuroda, *Chem. Commun.*, 1998, 559.
18 T. Kimura, Y. Sugahara and K. Kuroda, *Chem. Mater.*, 1999, **11**, 508.
19 Z. Luan, D. Zhao, H. He, J. Klinowski and L. Kevan, *J. Phys. Chem. B*, 1998, **102**, 1250.
20 Y. Z. Khimyak and J. Klinowski, *Phys. Chem. Chem. Phys.*, 2000, **2**, 5275.
21 Y. Z. Khimyak and J. Klinowski, *Chem. Mater.*, 1998, **10**, 2258.
22 Y. Z. Khimyak and J. Klinowski, *J. Chem. Soc., Faraday Trans.*, 1998, **94**, 2241.
23 Y. Z. Khimyak and J. Klinowski, *Phys. Chem. Chem. Phys.*, 2001, **3**, 616.
24 M. Schulz, M. Tiemann, M. Froba and C. Jäger, *J. Phys. Chem. B*, 2000, **104**, 10473.
25 J. Schaefer, E. O. Stejkal and R. Buchdahl, *Macromolecules*, 1977, **10**, 385.
26 S. Caldarelli, A. Meden and A. Tuel, *J. Phys. Chem. B*, 1999, **103**, 5477.
27 A. Steel, S. W. Carr and M. W. Anderson, *Chem. Mater.*, 1995, **7**, 1829.
28 K. Schmidt-Rohr and H. W. Spiess, *Multidimensional Solid-State NMR and Polymers*, Academic Press, London, 1994.